Catalysis Letters
https://doi.org/10.1007/s10562-021-03559-y

Pd/Mg(OH)$_2$ Heterogeneous Nanocatalysts Synthesized by a Facile One-Pot Hydrothermal Method for CO Direct Esterification to Dimethyl Oxalate

Xiao-Qi Lin[1,2] · Zhi-Qiao Wang[1] · Zhong-Ning Xu[1] · Guo-Cong Guo[1]

Received: 7 January 2021 / Accepted: 5 February 2021

Abstract

Pd-based heterogeneous nanocatalysts have wide application in chemical industry. However, the traditional synthesis process contains multi-steps such as impregnation, dry, calcination and reduction. The pre-synthesis nanoparticles process can reduce the steps, but need to remove the surfactants, which are added in the synthesis process. In this work, a facile one-pot hydrothermal synthesis process named as single molecular precursor method was successfully developed to prepare Pd/Mg(OH)$_2$ heterogeneous nanocatalysts with clean surface. The as-synthesized Pd/Mg(OH)$_2$ heterogeneous nanocatalysts show excellent performance for CO direct esterification to dimethyl oxalate (DMO). The WTY (weight time yield) of DMO can reach the high-performance of 2544 g $kg_{cat.}^{-1}$ h^{-1}, while the conversion of CO is 62.6% and selectivity to DMO is 90.8%. The single molecular precursor method developed by this work can be extended to other supported noble metal nanocatalysts.

✉ Zhi-Qiao Wang
842966248@qq.com

✉ Guo-Cong Guo
gcguo@fjirsm.ac.cn

[1] State Key Laboratory of Structural Chemistry, Fujian Institute of Research on the Structure of Matter, Chinese Academy of Sciences, Fuzhou 350002, Fujian, People's Republic of China

[2] University of Chinese Academy of Sciences, Beijing 100049, People's Republic of China

Published online: 27 February 2021

Graphic Abstract

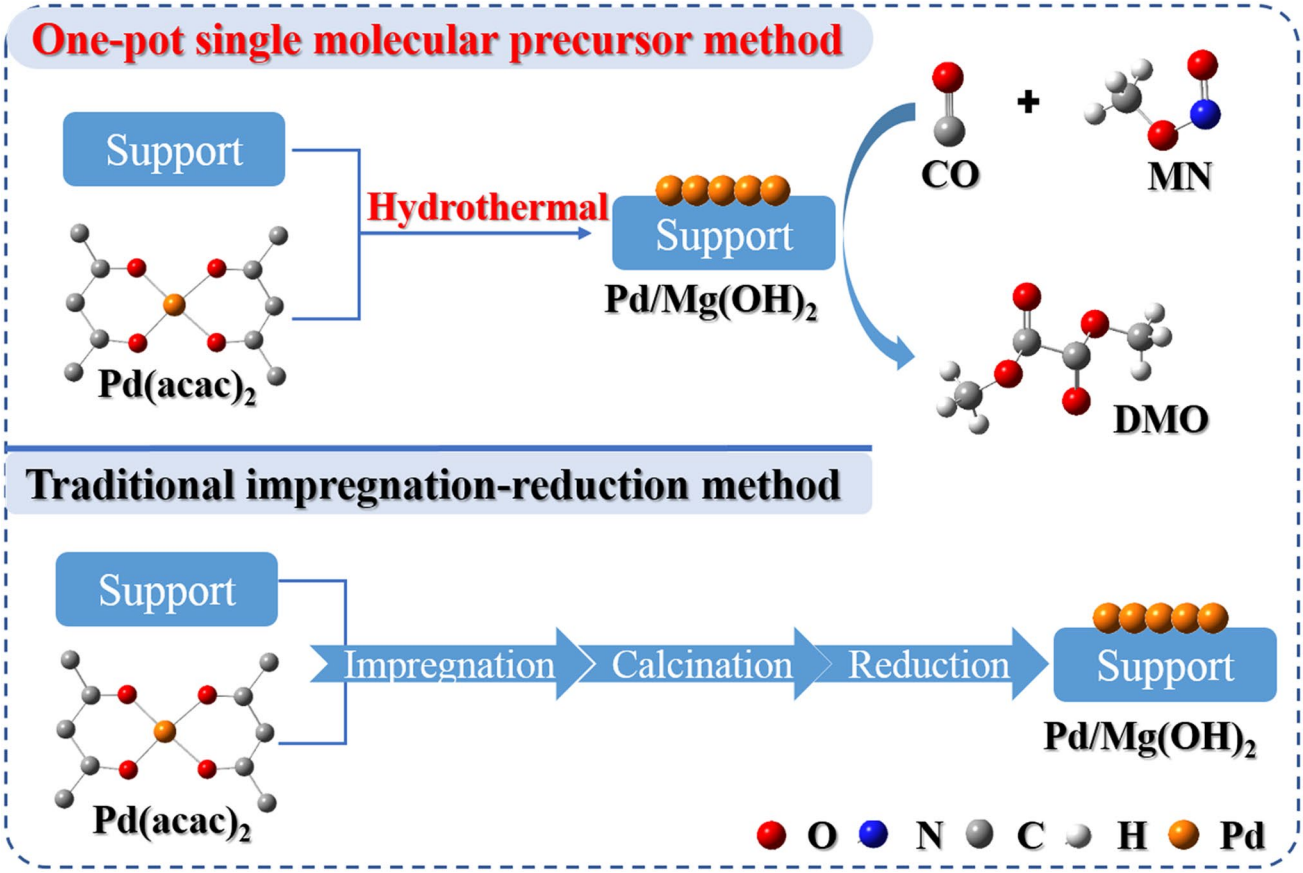

Keywords Heterogeneous nanocatalysts · Single molecular precursor method · CO direct esterification · Dimethyl oxalate

1 Introduction

Owing to its unique properties and broad applications, a research theme about noble-metal materials (e.g. Pd, Pt, Au) has been for decades [1]. It has played an important role in catalytic field, especially in heterogeneous catalytic processes, such as oxidation, hydrogenation/dehydrogenation, carbonylation, etc. [2–4]. Initially, Pd nanoparticles with uniform geometries or high-index facets were extensively studied [1, 5]. However, Pd nanoparticles with the small particle size and the large surface energy as catalysts are often unstable during catalytic application, leading to activity rapidly decays [3]. Several works have shown that this problem can be overcome by anchoring and highly dispersed the nanoparticles on the support as Pd-based heterogeneous nanocatalysts [6].

Increasing attention has been paid to the fabrication of Pd-based heterogeneous nanocatalysts, various synthetic methods have been proposed [7–10]. Among that, conventional wet impregnation and co-precipitation can easily lead to particles aggregation at elevated reaction temperatures [9]. Because of this, much work engaged in new synthetic strategies. Studies have shown that the introduction of organic compounds as surfactant agents or structure guide agents (such as cetyltrimethyl ammonium bromidecan (CTAB), poly-vinylpyrrolidone (PVP), polyethylene glycol (PEG), etc.) can control effectively the size and dispersion of Pd nanoparticles, namely pre-synthesis nanoparticles process [11–14]. Nevertheless, stabilizers that adsorbed strongly on the surface of active metal have been extremely limited in application due to contamination inevitably of the surface and resistance to reaction diffusion [12]. It is worth mentioning that the removal of the stabilizers is often accompanied by harsh post-treatments, which is extremely detrimental to the catalytic activity. What's worse, complete removal is almost impossible [14]. Recently, atomic layer deposition (ALD) has been demonstrated as an effective pathway for synthesizing Pd-based nanocatalysts without the use of surfactants [8, 15]. Interestingly, metal particles can be deposited directly on

the support through ALD and no post-treatment is encountered. Unfortunately, the chemisorption kinetics of the ALD metal precursor are relatively slow, easily leading to the sintering of metal species, thus affecting catalytic activity [8].

Dimethyl oxalate (DMO) is an important raw chemical, which usually is used for synthesizing oxalic acid and oxamide, etc. [15]. In the coal to ethylene glycol (EG) technology, EG is obtained from the hydrogenation of DMO, while DMO is synthesized from the CO direct esterification reaction [17]. CO direct esterification involves processes using CO as the starting material and ester chemicals (DMO, dimethyl carbonate (DMC) and methyl formate (MF), etc.) as products [16]. In traditional, it is reported that DMO can be obtained from the reaction of oxalic acid and alcohol [18]. However, the long production cycle limits the application. Compared with the conventional esterification method, CO direct esterification to DMO ($2CO + 2CH_3ONO = (COOCH_3)_2 + 2NO$, NO can be reused to prepare CH_3ONO) has drawn more and more attentions from scientists and researchers. As an important route to realize the transformation from inorganic carbon to organic carbon, CO direct esterification to DMO has been studied extensively. In recent years, Pd-based catalysts have been widely applied for CO direct esterification to DMO [13, 19]. Tremendous efforts have been devoted to the design of Pd-based heterogeneous nanocatalysts. However, several steps are needed for preparation, and surfactants and structural guide agents are introducing in the synthesis process, which is difficult to obtain Pd-based catalysts with clean surface. Based on this concept, a facile approach to prepare high-performance Pd-based heterogeneous nanocatalysts with clean surface is still a great challenge.

Herein, we provide a one-pot hydrothermal synthesis process named as single molecular precursor synthesis strategy to obtain Pd/Mg(OH)$_2$ heterogeneous nanocatalysts with clean surface. It analyzes through a variety of characterizations such as XRD, BET, XPS, HRTEM and in situ DRIRS. Under high temperature (180 °C) hydrothermal conditions, Mg(OH)$_2$ has been formed through reaction of MgO and boiling water. At the same time, Pd nanoparticles as active species could be easily introduced into the sample and obtain Pd/Mg(OH)$_2$ heterogeneous nanocatalysts, which takes palladium acetylacetone as single molecular precursor. The as-synthesized Pd/Mg(OH)$_2$ nanocatalysts show excellent performance for CO direct esterification to DMO. The WTY of DMO can reach the high-performance of 2544 g $kg_{cat.}^{-1}$ h^{-1}, while the conversion of CO is 62.6% and selectivity to DMO is 90.8%. Its preparation process is much facile compared to traditional impregnation-reduction method containing multi-steps. This work will provide a facile and effective way to preparation of high-performance supported nanocatalysts.

2 Experimental

2.1 Catalysts Preparation

C3 catalyst (denoted as **C3**) was prepared by one-pot single molecular precursor method. 0.0753 g palladium acetylacetone [Pd(acac)$_2$] was dissolved in 200 mL deionized water under stirred and ultrasound. 5 g of MgO was added in the palladium precursor solution with ultrasound for another 5 min. After that, the mixture was transferred to a 500 mL Teflon-lined steel autoclave and maintained at 180 °C for 12 h. After cooling the mixture to room temperature, the precipitate was centrifuged and washed with ultrapure water and ethyl alcohol several times and then dried at 80 °C for 12 h under vacuum. Meanwhile, **C1** and **C2** catalyst were also obtained by heat treatment during synthesis for 3 h and 5 h, respectively. For comparison, **C0-TI** catalyst (denoted as **C0-TI**) was prepared by traditional impregnation reduction method using Mg(OH)$_2$ as support and Pd(acac)$_2$ as palladium precursor. Details of the preparation procedures are present in the supplementary information (SI).

2.2 Catalysts Characterization

X-ray diffraction (XRD) patterns were recorded on a glass wafer by a Rigaku MiniFlex 600 diffractometer. Inductively Coupled Plasma (ICP) elemental analysis measurements were carried out on an Ultima2 spectrometer. The Brunauere–Emmette–Teller (BET) surface area is performed on ASAP 2020 instrument (Micromeritics). Samples for transmission electron microscopy (TEM) and high resolution TEM (HRTEM) observations were examined by a TEM (JEM-2010). X-ray photoelectron spectroscopy (XPS) measurements were taken with a VG Escalab 250 spectrometer equipped with an Al (Al-Kα = 1486.7 eV) anode and an Mg anode (Mg-Kα = 1253.6 eV). In situ diffuse reflectance infrared spectroscopy (DRIRS) measurements were performed on a Nicolet 6700 diffuse reflectance infrared spectrometer equipped with a stainless steel in situ IR flow cell.

2.3 Catalytic Activity Measurements

The catalytic activities of catalysts for CO direct esterification to DMO were evaluated on a fixed-bed quartz tubular reactor with 100 mg catalysts. The reactant gases include 28% CO, 20% CH_3ONO, 4% Ar as internal standard and 48% N_2 as the balance gas (weight hour space velocity (WHSV) about 6000 mL g^{-1} h^{-1}). The activity of catalyst

(CO conversion and DMO selectivity, see more details for SI) was evaluated under atmospheric pressure by an online Shimadzu GC-2014 gas chromatograph equipped with a thermal conductivity detector and a flame ionization detector.

3 Results and Discussions

We prepared **C1**, **C2** and **C3** catalysts by a one-pot single molecular precursor synthesis strategy with different heating time. As shown in Fig. S1, all the diffraction peaks matched well with $Mg(OH)_2$ phase (JCPDS: No. 07–0239), indicating that the MgO reacts with the boiling water in the system ($MgO + H_2O = Mg(OH)_2$ at 453 K). For comparison, **C0-TI** was synthesized by using the traditional wet-impregnation method with commercial $Mg(OH)_2$ support. It was found in Fig. 1 that the XRD patterns of **C3** and **C0-TI** catalysts could be attributed to the same crystalline phase. There is no obvious diffraction peak of Pd in all catalysts (Fig. 1 and Fig. S1), which suggests that the particle size of palladium is very small or very low crystallinity. By the ICP measurement, the Pd content in **C1**, **C2**, **C3** and **C0-TI** catalysts are 0.300%, 0.380%, 0.368%, 0.381%, respectively, which further confirms the above conjecture.

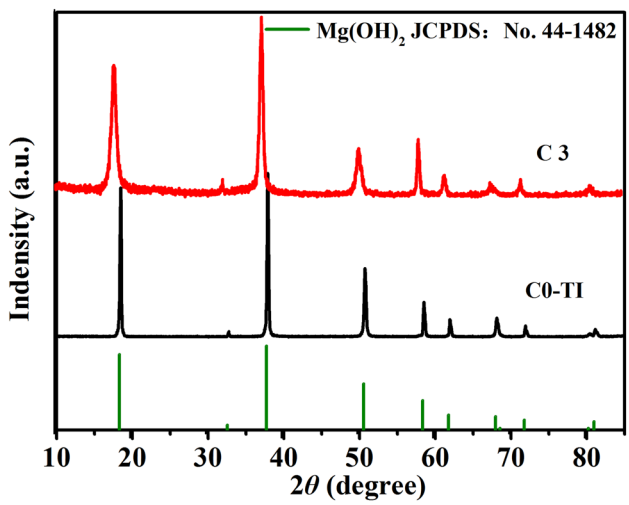

Fig. 1 PXRD patterns of **C3** and **C0-TI** catalysts**.** Vertical bars at the bottom denote the standard data for a brucite structure of $Mg(OH)_2$ (JCPDS: No. 07-0239)

It is worthy to mention that the morphologies of the synthetic and commercial samples are different, which can be revealed by the TEM images (Fig. S2). It can be seen that the commercial $Mg(OH)_2$ sample shows a lumpy shape, while **C3** is the thickness of $Mg(OH)_2$ nanosheets and it stacks to form a cluster of flowers, which may offer a high surface area for dispersing the metal. Physicochemical properties of catalysts are shown in Table S1. The surface area of **C1**, **C2** and **C3** catalysts was far higher than that of commercial $Mg(OH)_2$ (~ 80 vs. > 4 $m^2\ g^{-1}$, respectively, Table S1), offering the prospect of a higher density of anchor sites to immobilize metal atoms. The BET surface area of **C3** is higher than that of **C1**, **C2** and **C0-TI**, which is conducive to the full contact between reactants and catalysts and improves the catalytic performance.

HRTEM images presented in Fig. 2a and b reveal that the Pd nanoparticles of **C3** are highly dispersed on the $Mg(OH)_2$ support, while the Pd nanoparticles of **C0-TI** are somewhat aggregated into large nanoparticles during

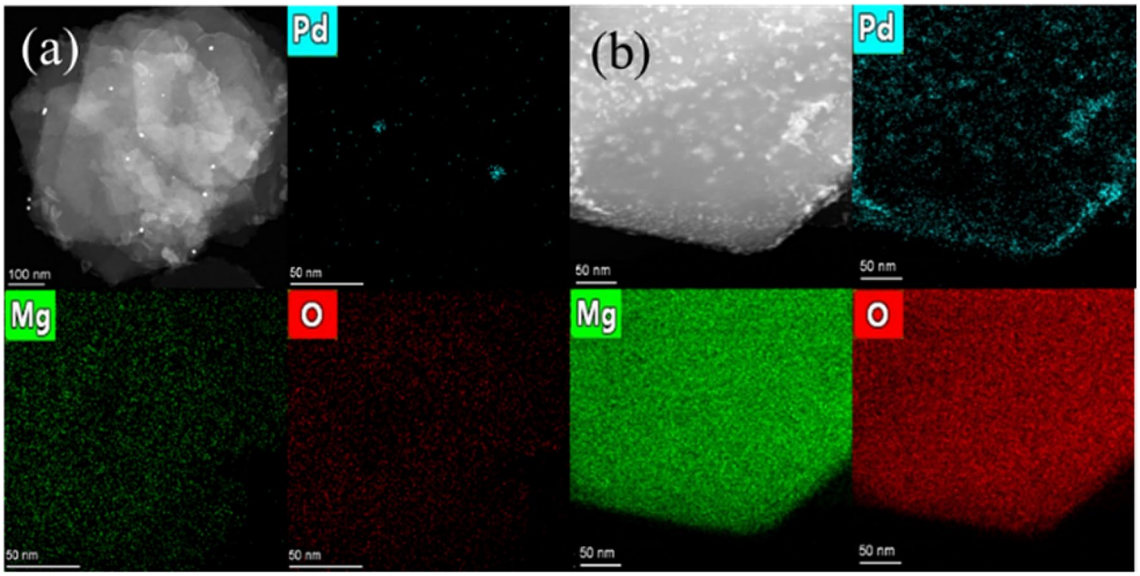

Fig. 2 HRTEM images of **C3** (**a**) and **C0-TI** catalysts (**b**), respectively

the catalyst preparation process. On the basis of the size distribution histograms shown in the insets of Fig. S3, Pd nanoparticles of **C3** revealed small Pd nanoparticles about 1.3 nm and a little Pd nanoparticles about 6 nm, which is much smaller than that of **C0-TI** (4.0–6.2 nm) as a whole. The TEM (Fig. S3a) images of **C1** showed that the large Pd nanoparticles are obvious with an average size approximate 8.7 nm. Similarly, the TEM (Fig. S3b) images of **C2** show that the average Pd size is about 6.6 nm, which is larger than that of **C0-TI** (4.0–6.2 nm). Previous reports have shown that the smaller size of the Pd active component facilitates the CO direct esterification reaction [13]. It illustrates that the catalytic activity of **C0-TI** is slightly higher than that of **C1** and **C2**, but lower than that of **C3** catalysts. Unfortunately, it is easily for Mg(OH)$_2$ support to be hydrolyzed by electron breakdown, leading to the observation of the Mg(OH)$_2$ support and the metal is not clear by TEM images. It was necessary to employ HRTEM and HRTEM-mapping in order to characterize the dispersion of the supported Pd on the Mg(OH)$_2$ support. Active component Pd could be clearly identified in the HRTEM image of **C3**, and the Pd nanoparticles were highly dispersed in the mapping results (Fig. 2). As a contrast, Pd particle size of **C0-TI** is obviously much bigger than that. Therefore, **C3** with much smaller particle size and much higher dispersion of Pd nanoparticles can easily account for the higher catalytic activity.

Figure S4 provides the XPS overview spectrum (Al Kα source) for **C3**. It can be seen from the figure that the position of the Mg 2p peak at 49.2 eV is attributed to the presence of Mg(OH)$_2$ [20]. This is consistent with the structure of XRD as mentioned above. Furthermore, the signal of Pd peak is difficult to detect as Mg KLL peak (300–350 eV) overlaps in the region of Pd 3d$_{5/2}$ peak and Pd loading is low. Hence, we further probe the Pd 3d peak using an Mg Kα radiation source, which can eliminate the effect of Mg KLL peak. In general, the peak around 335.0 eV assigns to Pd^0, while one around 337.0 eV assigns to Pd^{2+} [13]. When the heat treatment is only 3 h, the electron state of Pd over **C1** catalyst is still biased towards Pd^0 as two peaks at around 340.4 and 335.2 eV (Fig. S5), suggesting that the oxidation state of the Pd is mainly Pd^0. Pd(II) complexes with acetylacetonate as ligand have the characteristics of easy decomposition and good diffusion performance due to the introduction of acetylacetonate group [23]. During preparation via the single molecular precursor method, palladium acetylacetone as single molecular precursor is rapidly decomposed by heat to form Pd nanoparticles, which are deposited on the support [24]. While another two small peaks located at 342.1 and 336.0 eV are attributed to Pd$^{\delta+}$ ($0<\delta<2$). Indeed, it is likely that the obtained Pd nanoparticles showed characteristic of Pd$^{\delta+}$ species is due to the re-oxidation by adsorbing oxygen or hydroxyl groups on the surface of Mg(OH)$_2$ during the hydrothermal reaction

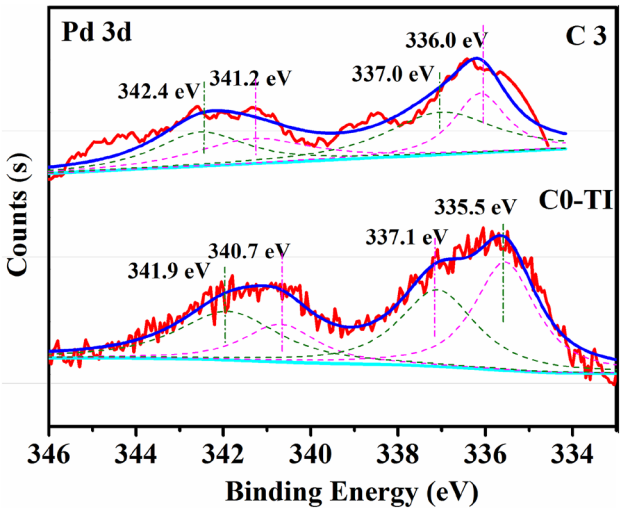

Fig. 3 Pd 3d XPS (Mg Kα source) spectra of **C3** and **C0-TI** catalysts

process [20]. Furthermore, the oxidized species increase with the extension of heat treatment time. Figure 3 offers ancillary evidence of the electronic state of Pd, revealing identical Pd 3d$_{5/2}$ binding energies of 336.0 eV for the **C3**, characteristic of Pd$^{\delta+}$ ($0<\delta<2$) species while Pd 3d$_{5/2}$ binding energies of 337.0 eV for the **C3**, characteristic of Pd^{2+} species. Moreover, one possible cause of producing partial Pd^{2+} is the surfaces of the catalysts are partially oxidized by the air during the characterization process [22]. Surface Pd$^{\delta+}$ species for CO direct esterification reaction are easily reduced to Pd^0 active component by CO, which further leads to the formation of DMO as main products [16]. Besides, the appearance of the two remaining peaks with binding energies of **C3** prepared by single molecular precursor method shifts higher than 340.7 and 335.5 eV of the **C0-TI** (Fig. 3). Based on the above experimental facts, we can infer that the introduction of a single molecular precursor method into the reaction system has a great influence on the interaction between metal and support, significantly increases the dispersion of active component Pd, and it also decreases the ensemble size of Pd nanoparticles over the **C3**.

Moreover, the interaction between the metal and support increases with the extension of the heat treatment time, which can improve CO adsorption and thus enhance catalytic activity [13]. CO adsorption can be further proved by in situ DRIRS of CO adsorption. As shown in Fig. 4, the peaks of 2019 cm^{-1} and 1925 cm^{-1} over **C3** catalyst are attributed to the bridge and linear adsorption of CO on the surface of the Pd species, respectively [21]. It can be observed that the broad peak of **C3** is still slightly higher than that of **C1** and **C2** from in situ DRIRS spectra of CO adsorption on **C1**, **C2**, **C3** catalysts (Fig. S6). CO adsorption peak of **C3** is the largest while there is only a small amount CO adsorbed in the **C0-TI** catalyst after N$_2$ sweeping. It

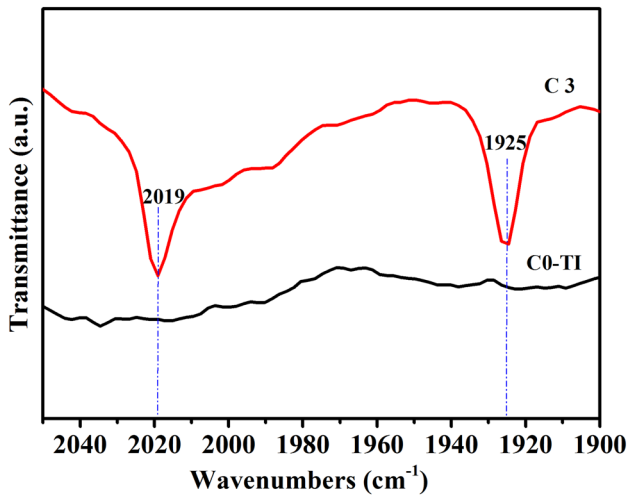

Fig. 4 In situ DRIRS spectra of CO adsorption on **C3** and **C0-TI** catalysts at 293 K in the range from 2050 to 1900 cm^{-1}

Table 1 The performances of **C3** and **C0-TI** catalysts used for CO direct esterification to DMO

Catalysts	Conversion of CO (%)	Selectivity to DMO (%)	WTY[a] (g $kg_{cat.}^{-1}$ h^{-1})
C3[b]	62.6	90.8	2544
C0-TI[c]	57.7	90.8	2347

Reaction conditions: 100 mg of catalyst, 6000 mL g^{-1} h^{-1} of weight hour space velocity (WHSV), reactants CO/CH_3NO volume ratio 1.4, 0.1 MPa, 403 K (for more details see SI)

[a]WTY represents the weight-time yield, grams of DMO per kilograms of catalyst per hour (g kg_{cat}^{-1} h^{-1})

[b]**C3** prepared with the heating time of 12 h

[c]**C0-TI** prepared with the traditional impregnation-reduction preparation

indicates that **C3** has a better CO adsorption and catalytic activities, which is consistent with the results of catalytic evaluation. Herein, we suggest that single molecular precursor method is an effective access to strength the interaction between metal and support and optimize the dispersion of active component Pd.

The evaluation of catalytic performance for CO direct esterification to DMO was carried out in a home-made catalytic evaluation device. **C0-TI** using traditional impregnation-reduction method were evaluated under the same reaction conditions as those that used a single molecular precursor method. As shown in Table 1, when used for CO direct esterification to DMO, the average WTY of DMO at the same reaction conditions demonstrate that the activity of **C3** shows better activity than **C0-TI**. It's noting worth that the catalytic performance improves as the heat treatment time increases (Table S2). CO conversion of **C3** can reach up to 62.6%, close to the theoretical maximum value of 71.4%. It implies that methyl nitrite was almost completely consumed, which can be verified using gas chromatography. What's more, the duration lifetime test of **C3** can be stable for at least 100 h at 403 K (Fig. S7) when it was applied to CO direct esterification to dimethyl oxalate. In addition, XRD patterns of **C3** before reaction and after reaction show no obvious diffraction peak of Pd species (Fig. S8). Even after use in the reaction, no obvious aggregation of Pd species was observed. This highly efficient and longlived nanocatalysts prepared via a facile one-pot single molecular precursor method may have a potential industrial application.

4 Conclusion

In summary, we developed a facile one-pot hydrothermal synthesis process named as single molecular precursor method to prepare Pd/$Mg(OH)_2$ heterogeneous nanocatalysts with clean surface. Notably, the as-synthesized Pd/$Mg(OH)_2$ heterogeneous nanocatalysts exhibits excellent performance when applied in CO direct esterification to DMO, and the WTY of DMO is 2544 g $kg_{cat.}^{-1}$ h^{-1}. The obtained catalysts were fully characterized by the XRD, BET, XPS, HRTEM and in situ DRIRS analyses. It was shown that, the single molecular precursor method has obvious superiority to the traditional impregnation-reduction method and pre-synthesis nanoparticles process. This new method can be extended to other supported noble metal nanocatalysts with clean surface.

Supplementary Information The online version of this article (https://doi.org/10.1007/s10562-021-03559-y) contains supplementary material, which is available to authorized users.

Acknowledgements This work was supported by the National Key Research and Development Program of China (2017YFA0206802, 2017YFA0700103, 2018YFA0704500), the Programs of the Chinese Academy of Sciences (QYZDJ-SSW-SLH028), the Natural Science Foundation of Fujian Province (2018J06005, 2018J05036).

Compliance with Ethical Standards

Conflict of interest The authors declare no conflict of interest.

References

1. Huang X, Zhao Z, Fan J et al (2011) Amine-assisted synthesis of concave polyhedral platinum nanocrystals having 411 high-index facets. J Am Chem Soc 133:34718–34721
2. Cai S, Rong H, Yu X et al (2013) Room temperature activation of oxygen by monodispersed metal nanoparticles: oxidative

dehydrogenative coupling of anilines for azobenzene syntheses. ACS Catal 3:478–486
3. Fu F, Xiang J, Cheng H et al (2017) A remarkably robust and efficient Pd_3 cluster catalyst for the Suzuki reaction and its odd mechanism. ACS Catal 7:1860–1867
4. Zhang Z, Dong Y, Wang L et al (2015) Scalable synthesis of a Pd nanoparticle loaded hierarchically porous graphene network through multiple synergistic interactions. ChemComm 51:8357–8360
5. Gao W, Hou Y, Hood ZD et al (2018) Direct in situ observation and analysis of the formation of palladium nanocrystals with high-index facets. Nano Lett 18:7004–7013
6. Wang H, Kong W, Zhu W et al (2014) One-step synthesis of Pd nanoparticles functionalized crystalline nanoporous CeO_2 and their application for solvent-free and aerobic oxidation of alcohols. Catal Comm 50:87–91
7. Li Z, Liu J, Huang Z et al (2013) One-pot synthesis of Pd nanoparticle catalysts supported on N-doped carbon and the application in the domino carbonylation. ACS Catal 3:839–845
8. Feng H, Libera JA, Stair PC et al (2011) Subnanometer palladium particles synthesized by atomic layer deposition. ACS Catal 1:665–673
9. Cheng N, Lv H, Wang W et al (2010) An ambient aqueous synthesis for highly dispersed and active Pd/C catalyst for formic acid electro-oxidation. J Power Sources 195:7246–7249
10. Park JN, Forman AJ, Tang W et al (2008) Highly active and sinter-resistant Pd-nanoparticle catalysts ecapsulated in silica. Small 4:1694–1697
11. Liu Y, Li Z, Yu Q et al (2019) A General Strategy for Fabricating Isolated Single Metal Atomic Site Catalysts in Y Zeolite. J Am Chem Soc 141:9305–9311
12. Rogers SM, Catlow CRA, Chan-Thaw CE et al (2017) Tandem site- and size-controlled Pd nanoparticles for the directed hydrogenation of furfural. ACS Catal 7:2266–2274
13. Xu ZN, Sun J, Lin CS et al (2013) High-performance and long-lived Pd nanocatalyst directed by shape effect for CO oxidative coupling to dimethyl oxalate. ACS Catal 3:118–122
14. Liu Y, Wang C, Wei Y et al (2011) Surfactant-induced postsynthetic modulation of Pd nanoparticle crystallinity. Nano Lett 11:1614–1617
15. Chen BR, Crosby LA, George C et al (2018) Morphology and CO oxidation activity of Pd nanoparticles on $SrTiO_3$ nanopolyhedra. ACS Catal 8:4751–4760
16. Wang ZQ, Sun J, Xu ZN et al (2020) CO direct esterification to dimethyl oxalate and dimethyl carbonate: the key functional motifs for catalytic selectivity. Nanoscale 12:20131–20140
17. Yue H, Zhao Y, Ma X et al (2012) Ethylene glycol: properties, synthesis, and applications. Chem Soc Rev 41:4218–4244
18. Funakawa A, Yamanaka I, Takenaka S et al (2004) Selectivity control of carbonylation of methanol to dimethyl oxalate and dimethyl carbonate over gold anode by electrochemical potential. J Am Chem Soc 126:5346–5347
19. Lin Q, Ji Y, Jiang ZD et al (2007) Effects of precursors on preparation of Pd/γ-alumina catalyst for synthesis of dimethyl oxalate. Ind Eng Chem Res 46:7950–7954
20. Claus P, Berndt H, Mohr C et al (2000) Pd/MgO: catalyst characterization and phenol hydrogenation activity. J Catal 192:88–97
21. Wang C, Chen P, Li Y et al (2016) In situ DRIFTS study of CO coupling to dimethyl oxalate over structured Al-fiber@ns-AlOOH@Pd catalyst. J Catal 344:173–183
22. Guadix-Montero S, Alshammari H, Dalebout R et al (2017) Deactivation studies of bimetallic AuPd nanoparticles supported on MgO during selective aerobic oxidation of alcohols. Appl Catal A: Gen 546:58–66
23. Xomeritakis G, Lin YS (1998) CVD synthesis and gas permeation properties of thin palladiurn/alurnina membranes. AIChE J 44:174–177
24. Liang G, Gao WG, Liu WP et al (2006) Thermal behavior of palladium(II) acetylacetonate. Rare Metal Mat Eng 35:150–153